Supplementary Data

Communicated to: *Dalton Trans*
Manuscript Type : Article
Manuscript ID : DT-ART-09-2013-052518-R1

Mixed Ligand μ-Phenoxo-bridged Dinuclear Copper(II) Complexes with Diimine Co-ligands: Efficient Chemical Nuclease and Protease Activities and Cytotoxicity

Rangasamy Loganathan,[a] Sethu Ramakrishnan,[b] Eringathodi Suresh,[c] Mallayan Palaniandavar[a]* Anvarbatcha Riyasdeen,[d] and Mohamad Abdulkadhar Akbarsha[e,f]

[a]*Department of Chemistry, Central University of Tamil Nadu,Thiruvarur 610004, Tamil Nadu, India*
[b]*School of Chemistry, Bharathidasan University, Tiruchirappalli – 620 024, Tamil Nadu, India*
[c]*Analytical Science Discipline, Central Salt and Marine Chemical Research Institute, Bhavnagar 364 002, India*
[d]*Department of Animal Science, Bharathidasan University, Tiruchirappalli – 620 024, Tamil Nadu, India*
[e]*Mahatma Gandhi-Doerenkamp Center for Alternatives to use of Animals in Life Science Education, Bharathidasan University, Tiruchirappalli, 620024, Tamil Nadu, India*
[f]*Visiting Professor, Department of Food Sciences and Nutrition, College of Food Sciences and Agriculture, King Saud University, Riyadh-11451, Kingdom of Saudi Arabia*

*Author to whom correspondence should be addressed *e-mail*: palaniandavarm@gmail.com, palanim51@yahoo.com

Description of Crystal Structure of $[Cu(sal)(bpy)(ClO_4)]_2$ 1

The bond distances and bond angles observed for $[Cu(sal)(bpy)(ClO_4)]_2$ **1** are in the same ranges as observed for $[Cu(sal)(bpyam)(ClO_4)]_2$,[59] [Cu(sal)(acetylphenolato)$(ClO_4)]_2$,[60] [Cu(3-methoxysalicylaldiminato)(bpy)$(ClO_4)]_2$,[58] [Cu(4-methoxysalicylaldiminato)(bpy)$(ClO_4)]_2$,[58] [Cu(5-carboxysalicyaldehydato)(bpy)$(ClO_4)]$,[61] [Cu(5-carboxysalicylaldehydato)(bpy)$(H_2O)]_2$,[61] and [Cu(sal)(acetylphenolato)$(NO_3)]$.[62] Also, they are in good agreement with the monomeric copper(II) complex [Cu(salicylate)(bpy)]·EtOH·H_2O.[63]

Description of Crystal Structure of $[Cu(sal)(phen)(ClO_4)]_2$ 2

The bond distances and bond angles observed for $[Cu(sal)(phen)(ClO_4)]_2$ **2** are in the same ranges as observed for the same complex reported already.[64-66] Also, they are in good agreement with [Cu(sal)(4,7-diphenylphen)$(H_2O)]_2$[67] and [Cu(MeOsalicylate)(phen)], where H(MeOsalicylate) is methoxysalicylic acid.[68]

Description of Crystal Structure of $[Cu(sal)(phen)(NO_3)]_2$ 2a

The centrosymmetric dimeric structure of **2a** is similar to that of **2.** Upon replacing the perchlorate anion in **2** by nitrate anion to obtain **2a**, negligible changes are observed in the equatorial Cu-N_{imine}, Cu-$O1_{phenolate}$ and Cu-$O2_{carbonyl}$ bond distances. The axial bond Cu-O3 (2.3795(16) Å) involving the oxygen atom of nitrate group in **2a** is longer than the equatorial bonds, which is expected of the presence of two electrons in the d_{z^2} orbital of Cu(II). Interestingly, the tetragonality[16] of **2a** (T, 0.763)[16,64] is lower than that (T, 0.783) of the perchlorate analogue **2** suggesting that the presence of perchlorate anion leads to a higher static stereochemical distortion. The Cu...Cu separation in **2a** (3.471 Å) is longer than that **2** indicating that the interaction between the two metal centers in the former is weaker. This is supported by the lower O-Cu-O bond angle (168.92(5)°) and smaller Cu–O–Cu bridge angle (94.48°) revealing that the extent of antiferromagnetic interaction in **2a** is stronger than that in **2**.[58]

DNA Binding Studies: UV-Vis Absorption and Emission Spectral Titrations.

The DNA binding affinities of the complexes varying as **5** > **4** > **3** > **2** ~ **2a** > **1**, which is the same as that for the observed decrease in order of hypochromism. Similar observations have been made by us earlier for the mononuclear tris-diimine complexes $[Cu(5,6\text{-dmp})_3]^{2+}$, $[Zn(5,6\text{-dmp})_3]^{2+}$ [56] and $[Ru(5,6\text{-dmp})_3]^{2+}$,[75] the mixed ligand complexes $[Ru(NH_3)_4(5,6\text{-dmp})]^{2+}$,[76] [Cu(imda)(5,6-dmp)],[31] $[Cu(dipica)(5,6\text{-dmp})]^{2+}$,[77] $[Cu(pmdt)(5,6\text{-dmp})]^{2+}$,[15] $[Cu(bba)(5,6\text{-dmp})]^{2+}$ [15] and $[Cu(L\text{-tyr})(5,6\text{-dmp})]^{+}$ [15] and the dinuclear complexes $[\{(5,6\text{-dmp})_2Ru\}_2(bpm)]^{4+}$ [78] and $[Cu_2(LH)_2(5,6\text{-dmp})(ClO_4)_2]^{2+}$ [16] bound to CT DNA, all of them containing 5,6-dmp as the co-ligand, and $[Cu(tdp)(3,4,7,8\text{-tmp})]^{2+}$.[14]

Circular Dichrosim Spectral Studies.

Similar B to A conformational change have been observed by us earlier for mixed ligand[31,76-78] mono-[56,75-77] and dinuclear[16] complexes of 5,6-dmp ligand bound to CT DNA. Similar to **3**, **4** also exhibits a red-shift (14 nm) with a large decrease in intensity of the DNA helicity band and a red-shift (14 nm) with increase in intensity of the positive band (**Figure 4**), which is consistent with a B to A conformational change of DNA on binding of the complex with the four methyl groups on 3,4,7,8-tmp co-ligand effectively placed in DNA grooves. Similar observations made for $[Cu(tdp)(3,4,7,8\text{-tmp})]^{+}$ complexes bound to CT DNA have been ascribed to B to A conformational change.[14]

Table S1 Electronic absorption[a] spectral properties of Cu(II) complexes

Complex	λ_{max}, nm (ε, M^{-1} cm^{-1})		
	Ligand field[b]	LMCT[c]	Ligand based[d]
[Cu(sal)(bpy)]$^+$ **1**	645(160)	372 (4560)	300(32130)
[Cu(sal)(phen)]$^+$ **2**	638(100)	383(2540)	273(24990)
[Cu(sal)(phen)]$^+$ **2a**	636(130)	372 (4620)	269(25820)
[Cu(sal)(5,6-dmp)]$^+$ **3**	632 (170)	380 (3530)	278 (29810)
[Cu(sal)(3,4,7,8-tmp)]$^+$ **4**	628 (160)	384 (3710)	279 (28440)
[Cu(sal)(dpq)]$^+$ **5**	661 (90)	383 (4750)	259 (18530)

[a]In 5 mM Tris-HCl/50 mM NaCl buffer solution at pH 7.1

[b]Concentration, 5×10^{-3} M, [c]Concentration, 2×10^{-5} M, [d]Concentration, 100×10^{-5} M

Table S2 EPR spectral properties of Cu(II) complexes

Complex	$g_{\|}$	$A_{\|}$ (10^{-4} cm^{-1})	$g_{\|}A_{\|}$ (cm)	$g_{\perp}$
[Cu(sal)(bpy)]$^+$ **1**	2.228	181	123	2.047
[Cu(sal)(phen)]$^+$ **2**	2.235	182	123	2.047
[Cu(sal)(phen)]$^+$ **2a**	2.231	181	123	2.045
[Cu(sal)(5,6-dmp)]$^+$ **3**	2.234	180	124	2.056
[Cu(sal)(3,4,7,8-tmp)]$^+$ **4**	2.235	183	122	2.052
[Cu(sal)(dpq)]$^+$ **5**	2.232	190	117	2.050

[b]In 5 mM Tris-HCl/50 mM NaCl buffer (pH 7.1):acetone (4:1 V/V) glass at 77 K

Table S3 Electrochemical data of Cu(II) complexes

Complex		E_{pa} (V)	E_{pc} (V)	ΔE_p (V)	$E_{1/2}$ (V) CV[a]	$E_{1/2}$ (V) DPV[b]
$[Cu(sal)(bpy)]^+$	**1**	-0.100	-0.230	0.130	-0.165	-0.160
$[Cu(sal)(phen)]^+$	**2**	-0.090	-0.170	0.080	-0.130	-0.134
$[Cu(sal)(5,6\text{-dmp})]^+$	**3**	-0.096	-0.210	0.114	-0.153	-0.154
$[Cu(sal)(3,4,7,8\text{-tmp})]^+$	**4**	-0.070	-0.230	0.160	-0.150	-0.145
$[Cu(sal)(dpq)]^+$	**5**	-0.020	-0.152	0.132	-0.086	-0.077

[a]Measured *vs.*non-aqueous Ag/Ag^+ reference electrode; add 544 mV [300 mV, Ag/Ag^+ to SCE + 244 mV, SCE to SHE] to convert to standard hydrogen electrode (SHE); Fc/Fc^+ couple, $E_{1/2}$, 0.039 V (CV); 0.042 (DPV), Scan rate 50 mV s^{-1}; Supporting electrolyte, *Tetra-N*-butylammonium perchlorate (0.1 mol dm^{-3}); Complex concentration, 1 mmol.dm^{-3};

[b]Differential Pulse Voltammetry, scan rate 5 mVs^{-1}; pulse height 25 mV.

a

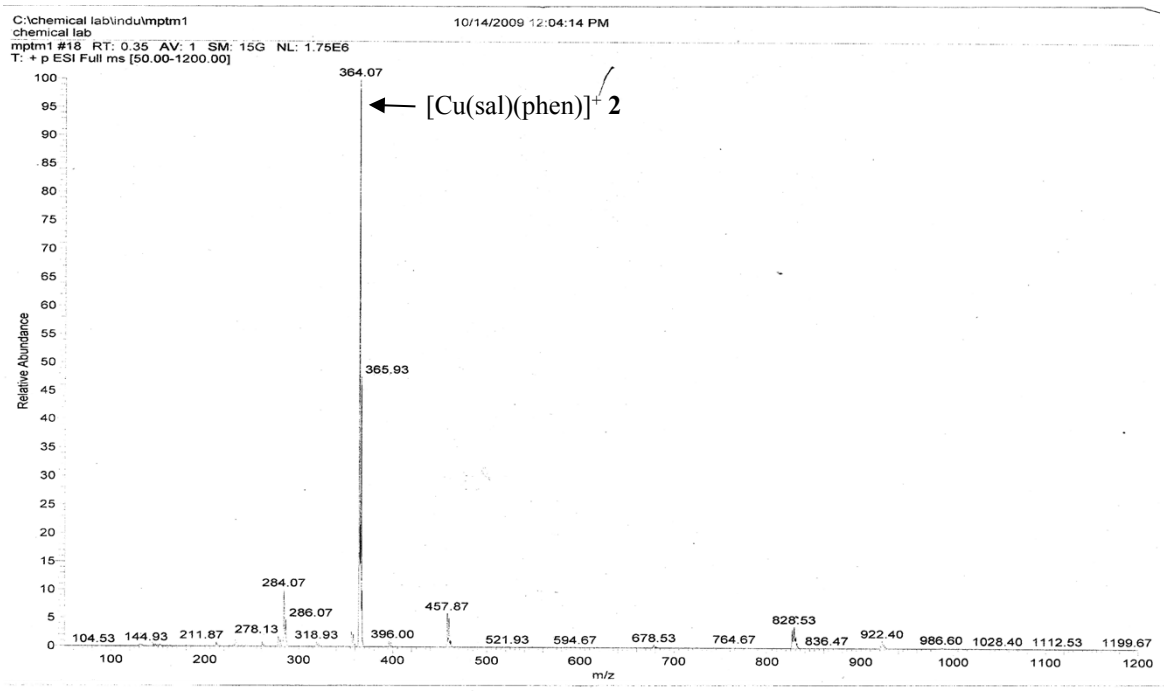

b

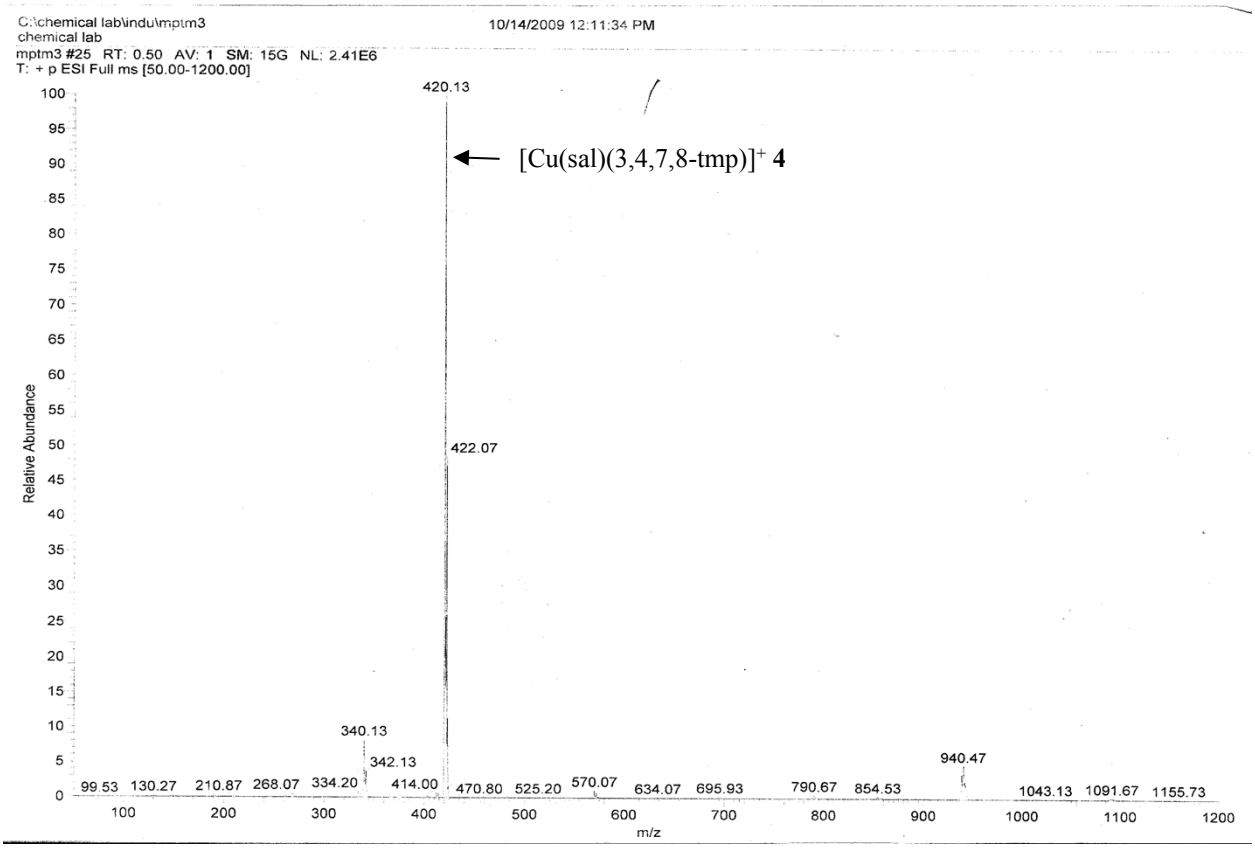

Figure S1 ESI-MS spectra of $[Cu(sal)(phen)]^+$ **2** (a) and $[Cu(sal)(3,4,7,8\text{-tmp})]^+$ **4** (b) in acetonitrile

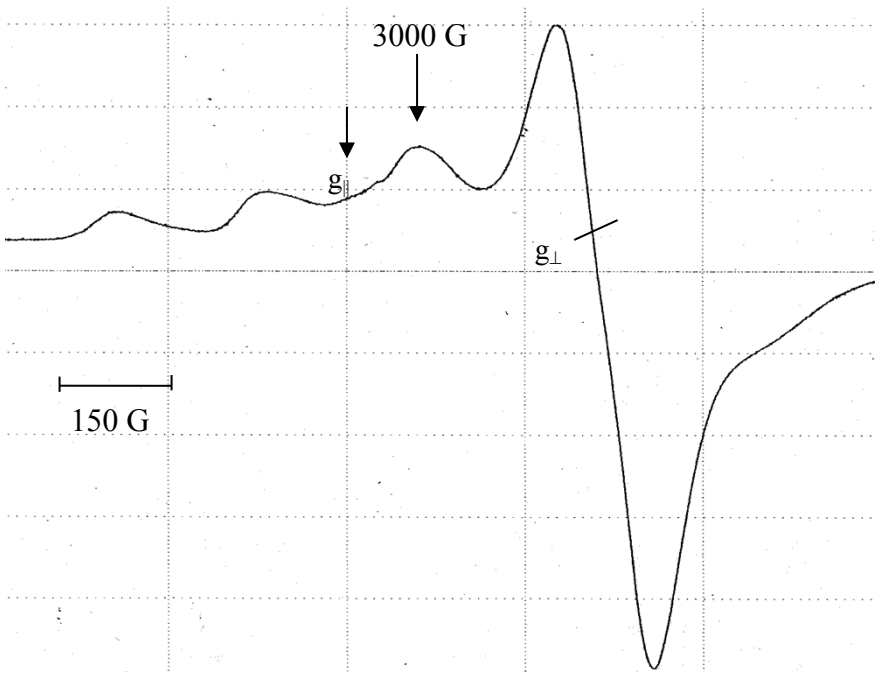

Figure S2 X-band EPR spectra of $[Cu(sal)(phen)]^+$ **2** in 5 mM Tris-HCl/50 mM NaCl buffer (pH 7.1):acetone (4:1 v/v) glass at 77 K. Microwave frequency 9.0753 GHz

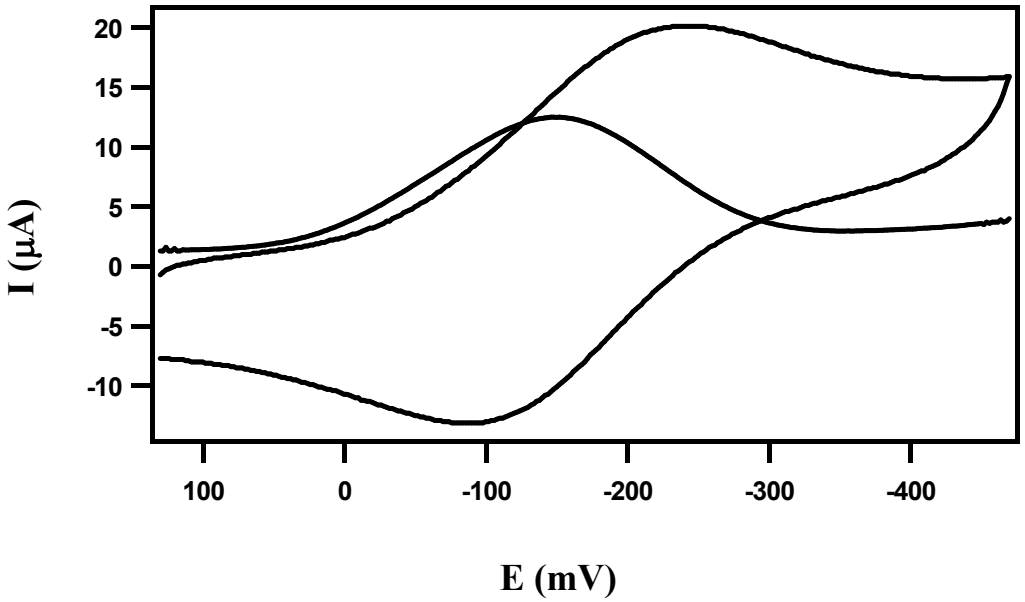

Figure S3 Cyclic and differential pulse voltammograms of $[Cu(sal)(phen)]^+$ **2** (0.5 mM) in acetonitrile at 25 ^{0}C at 50 mVs^{-1} and 5 mVs^{-1} scan rate respectively

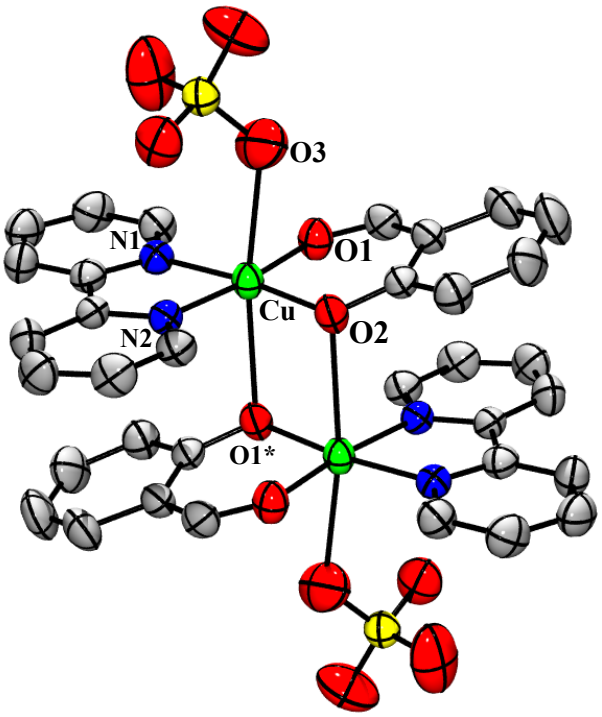

Figure S4 ORTEP view of $[Cu(sal)(bpy)(ClO)_4]_2$ **1** showing atom numbering scheme and displacement ellipsoids (50% probability level)

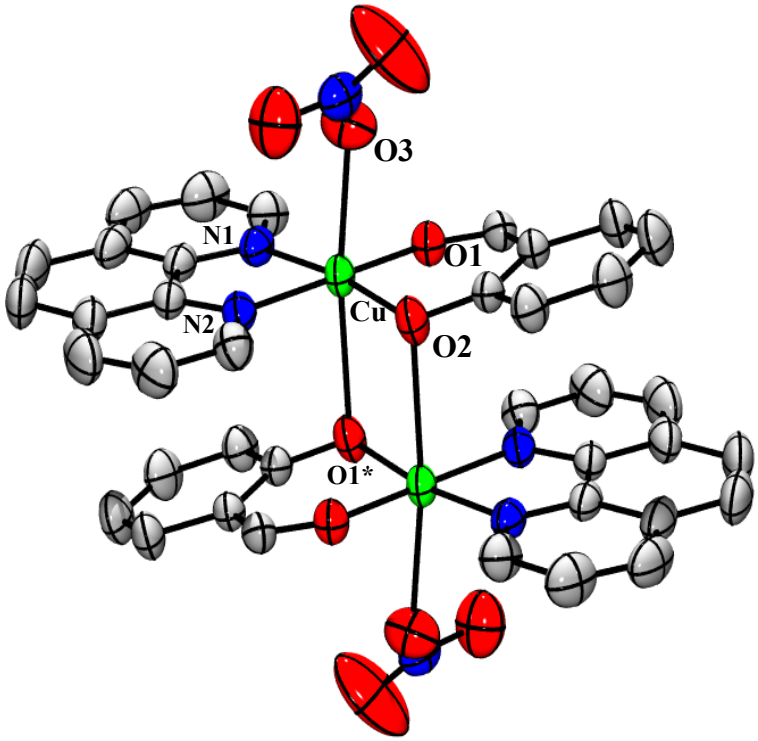

Figure S5 ORTEP view of $[Cu(sal)(phen)(NO)_3]_2$ **2a** showing atom numbering scheme and displacement ellipsoids (50% probability level)

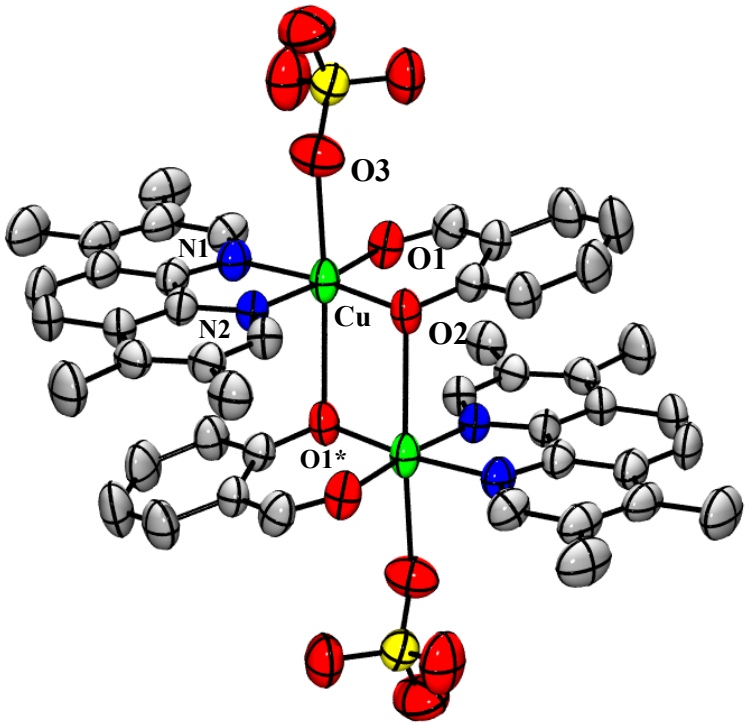

Figure S6 ORTEP view of $[Cu(sal)(3,4,7,8\text{-tmp})(ClO)_4]_2$ **4** showing atom numbering scheme and displacement ellipsoids (50% probability level)

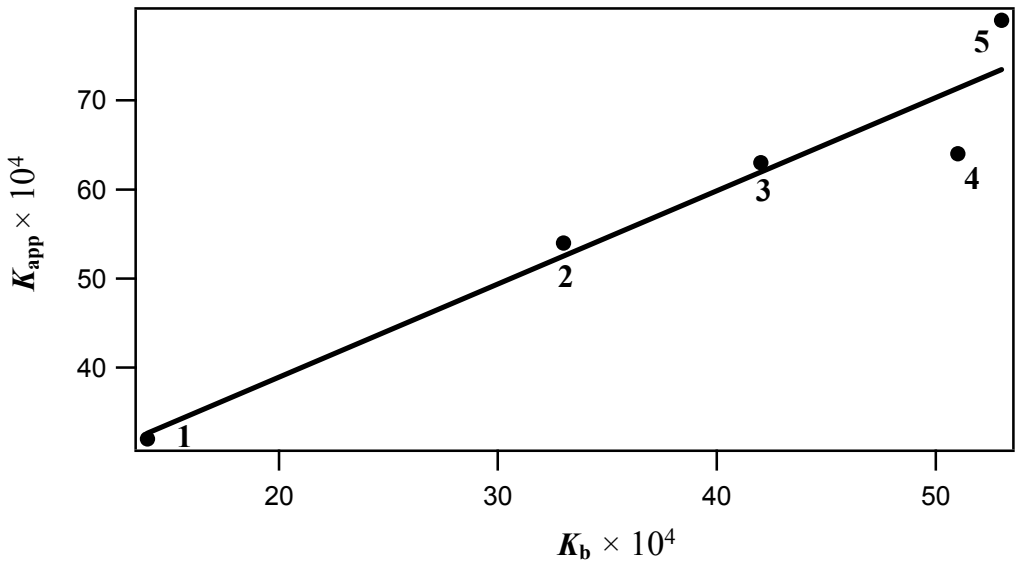

Figure S7 Plot of K_{app} *vs* K_b

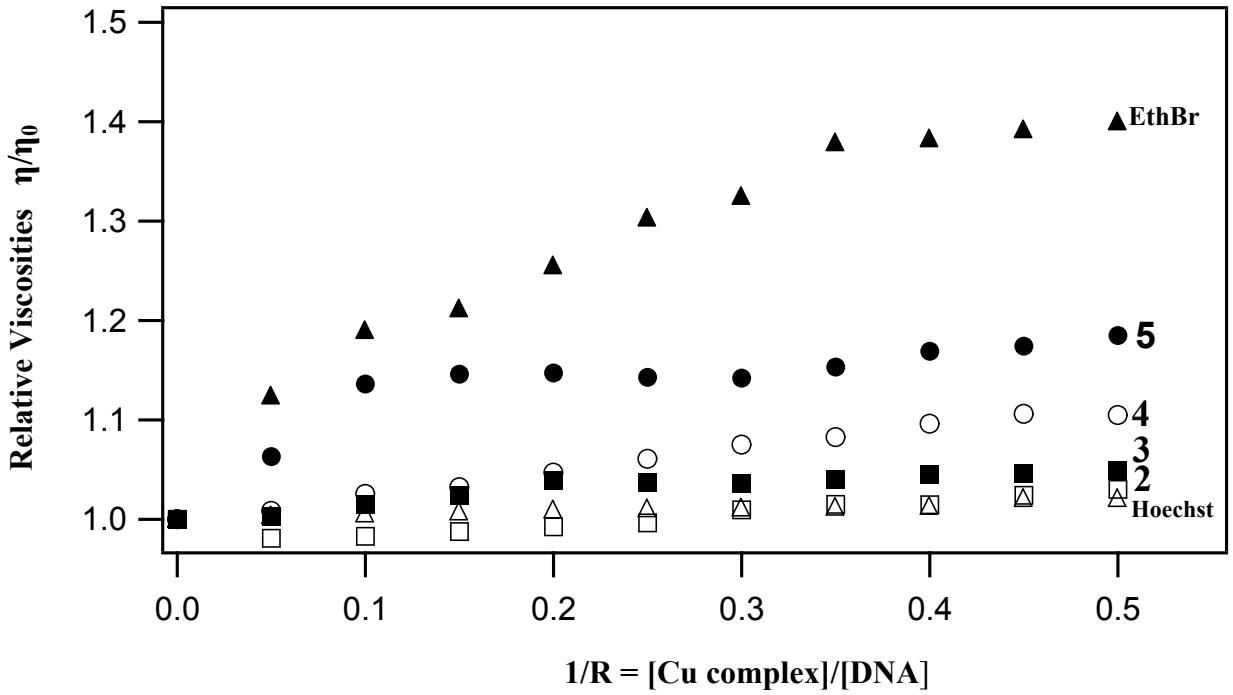

Figure S8 Effect of addition of complexes $[Cu(sal)(phen)(ClO_4)_2]_2$ (**2**), $[Cu(sal)(5,6\text{-}dmp)(ClO_4)_2]_2$ (**3**), $[Cu(sal)(3,4,7,8\text{-}tmp)(ClO_4)_2]_2$ (**4**), $[Cu(sal)(dpq)(ClO_4)_2]_2$ (**5**) to CT DNA; The relative viscosities *vs* 1/ R; [CT DNA] = 500 μM. The ethidium bromide and Hoechst were used as control for standard intercalator and groove binding agent, respectivey.

A

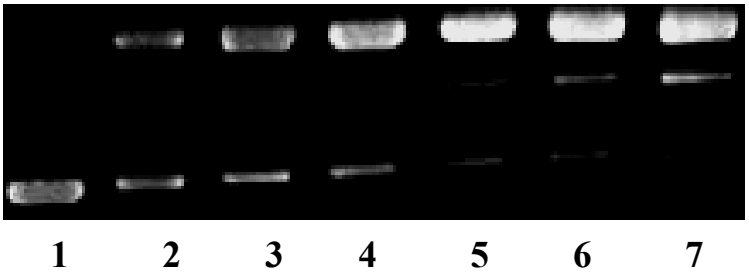

Figure S9A The cleavage of supercoiled pUC19 DNA (40 μM) by complexes **1 – 5** (80 μM) with incubation time of 1 h in 5 mM Tris-HCl/50 mM NaCl buffer at pH 7.1. Lane 1, DNA control; Lane 2, DNA + $Cu(ClO_4)_2 \cdot 6H_2O$; Lane 3, DNA + **1**; Lane 4, DNA + **2**; Lane 5, DNA + **3**; Lane 6, DNA + **4**; Lane 7, DNA + **5**. Forms SC, NC and LC are Supercoiled, Nicked Circular and Linear Circular DNA respectively

B

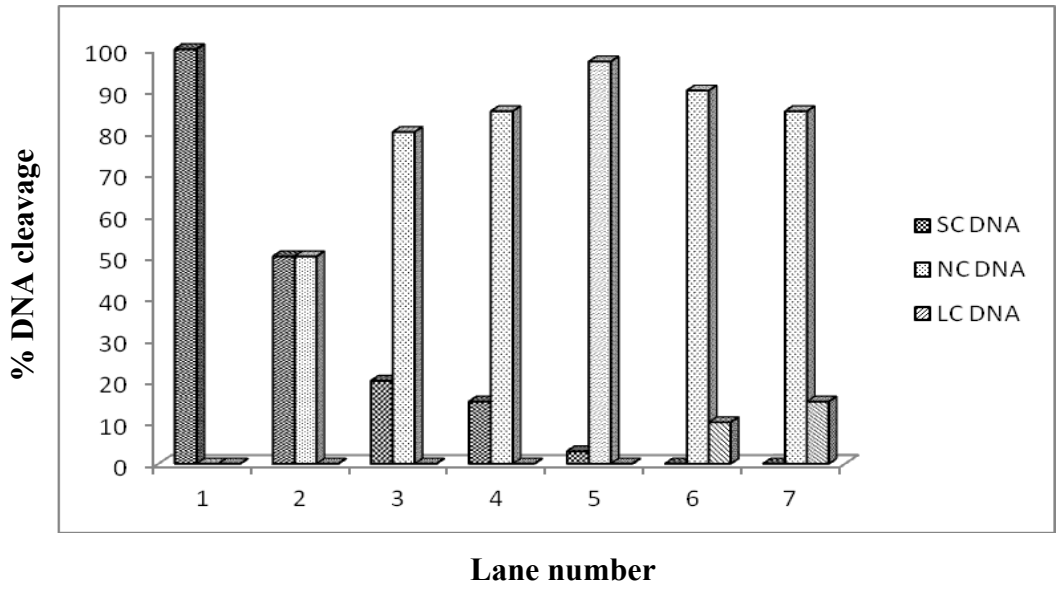

Figure S9B Plot shows % DNA cleavage *vs.* complexes **1 - 5** (100 μM, lane 3 – 7) for an incubation period of 1 h

A

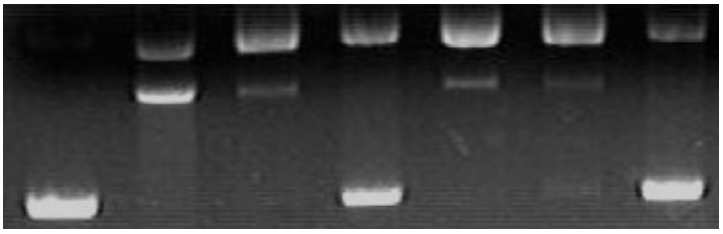

Figure S10A Gel electrophoresis diagram of cleavage of supercoiled pUC19 DNA (40 μM) by the complex **5** (80 μM) in 5 mM Tris-HCl/50 mM NaCl at pH = 7.1 and in the presence of different additives at 37 ^{o}C. Lane 1, DNA; Lane 2, DNA + **5**; Lane 3, DNA + **5** + NaN_3 (100 μM); Lane 4, DNA + **5** + DMSO (6 μL); Lane 5, DNA + **5** + SOD (4 unit); Lane 6, DNA + **5** + Catalase (10 unit); Lane 7, DNA + **5** + Ethanol (6 μL). Forms SC, NC and LC are Supercoiled, Nicked Circular and Linear Circular DNA respectively

B

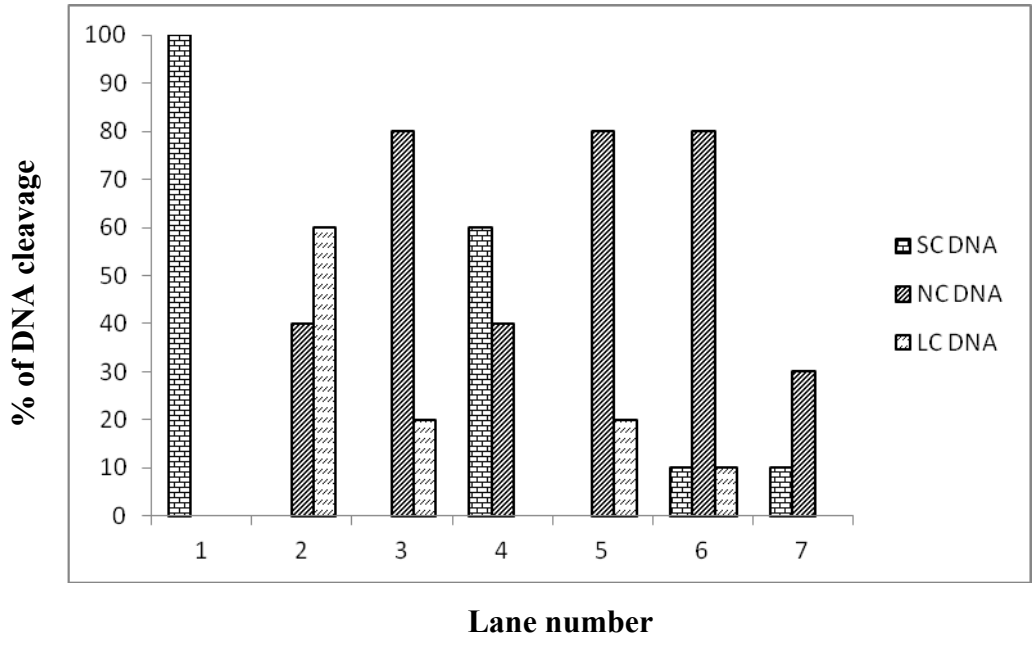

Figure S10B Bar diagram showing the relative amounts of the different DNA forms in the presence of complex **5** and different additives

A

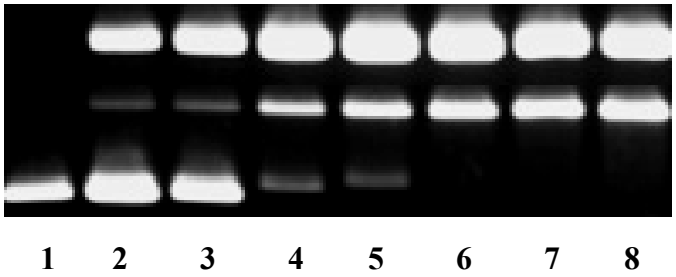

Figure 11A Gel electrophoresis diagram of cleavage of supercoiled pUC19 DNA (40 μM) by using various concentrations of complex **5** in a 5 mM Tris-HCl/50 mM NaCl at pH = 7.1 and in the presence of ascorbic acid (H_2A, 10 μM) at 37 ^oC for 1 h. Lane 1, DNA + H_2A; Lane 2, DNA + H_2A + **5** (5 μM); Lane 3, DNA + H_2A + **5** (10 μM); Lane 4, DNA + H_2A + **5** (15 μM); Lane 5, DNA + H_2A + **5** (20 μM); Lane 6, DNA + H_2A + **5** (30 μM); Lane 7, DNA + H_2A + **5** (40 μM); Lane 8, DNA + H_2A + **5** (50 μM). Forms SC, NC and LC are Supercoiled, Nicked Circular and Linear Circular DNA respectively

B

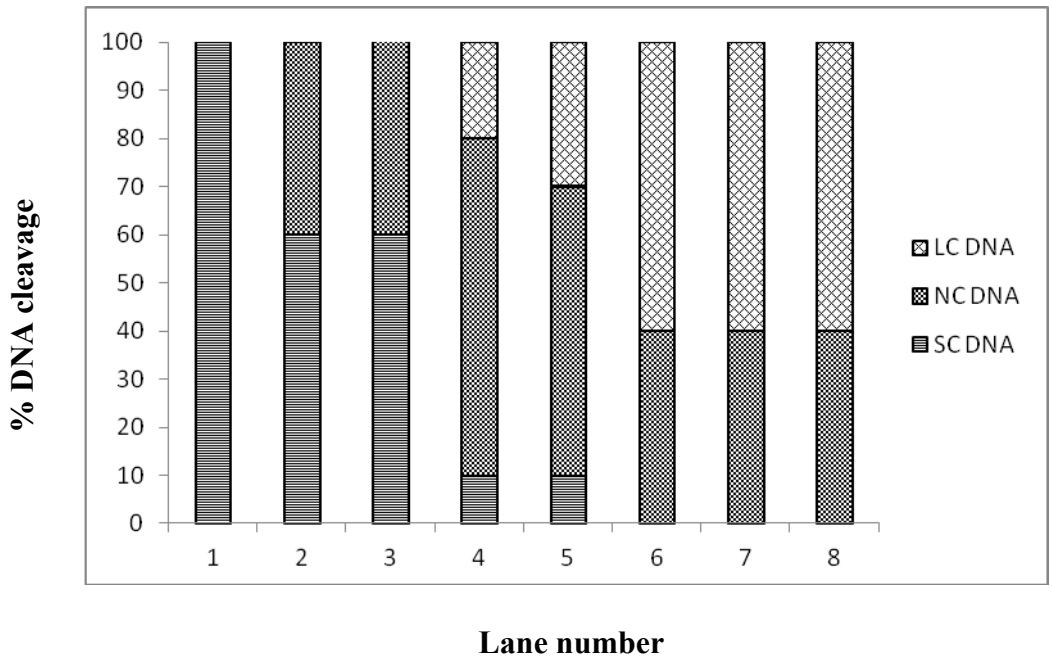

Figure 11B Plot shows concentration dependent oxidative cleavage of supercoiled pUC19 DNA with different complex concentrations of **5** (5 – 50 μM) for 1 h

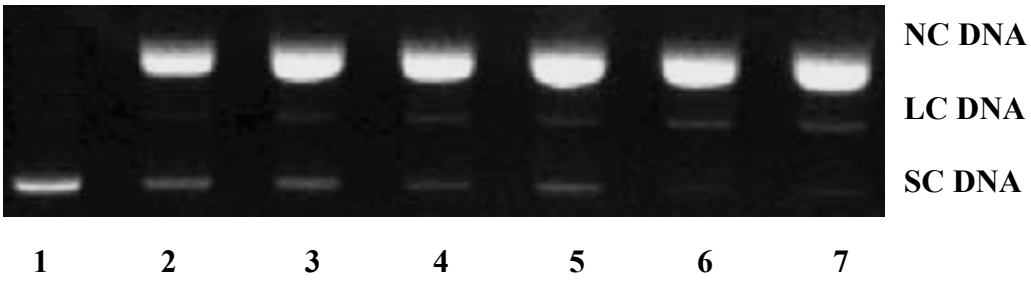

Figure S12A Time dependent cleavage of supercoiled pUC19 DNA (40 μM) by the complex **5** (100 μM) in 5 mM Tris-HCl/50 mM NaCl at pH = 7.1 and at 37 ^{o}C Lane 1, DNA; Lane 2, DNA + **5** (10 min); Lane 3, DNA + **5** (20 min); Lane 4, DNA + **5** (30 min); Lane 5, DNA + **5** (40 min); Lane 6, DNA + **5** (50 min); Lane 7, DNA + **5** (60 min). Forms SC, NC and LC are Supercoiled, Nicked Circular and Linear Circular DNA respectively

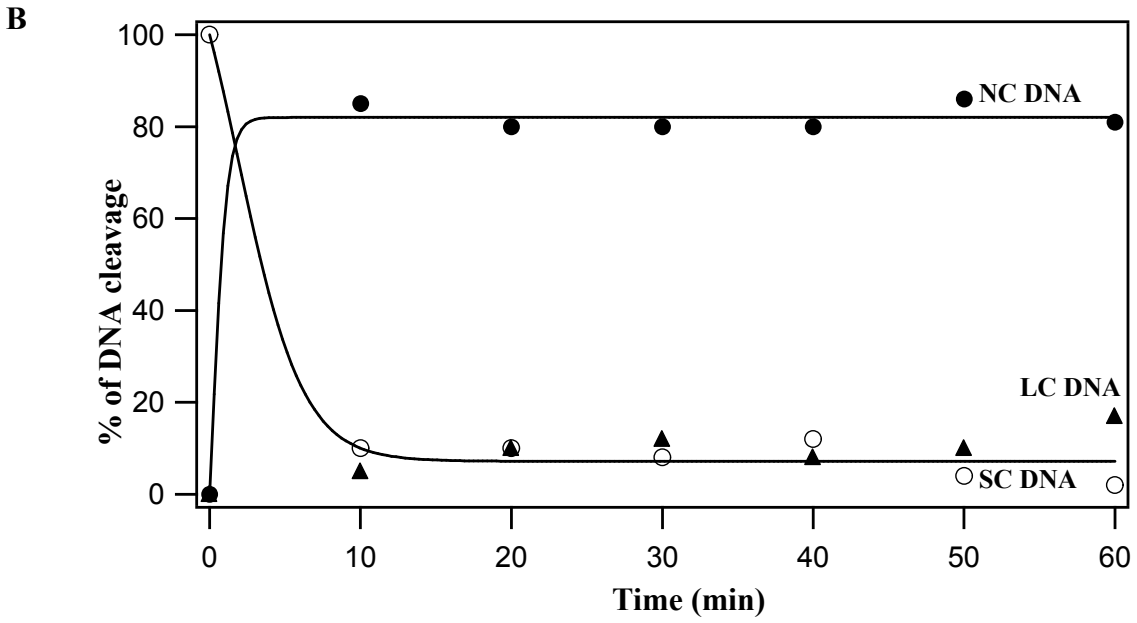

Figure S12B Plot shows % DNA cleavage *vs.* time of incubation (0 – 60 min) for complex **5** (100 μM)

Figure S13 Gel electrophoresis diagram of cleavage of supercoiled pUC19 DNA (40 μM) by using various concentrations of complex **4** in a 5 mM Tris-HCl/50 mM NaCl at pH = 7.1 and in the presence of ascorbic acid (H_2A, 10 μM) at 37 ^oC for 1 h. Lane 1, DNA + H_2A; Lane 2, DNA + H_2A + **4** (10 μM); Lane 3, DNA + H_2A + **4** (20 μM) ; Lane 4, DNA + H_2A + **4** (30 μM); Lane 5, DNA + H_2A + **4** (40 μM); Lane 6, DNA + H_2A + **4** (50 μM); Lane 7, DNA + H_2A + **4** (60 μM); Lane 8, DNA + H_2A + **4** (80 μM). Forms SC, NC and LC are Supercoiled, Nicked Circular and Linear Circular DNA respectively

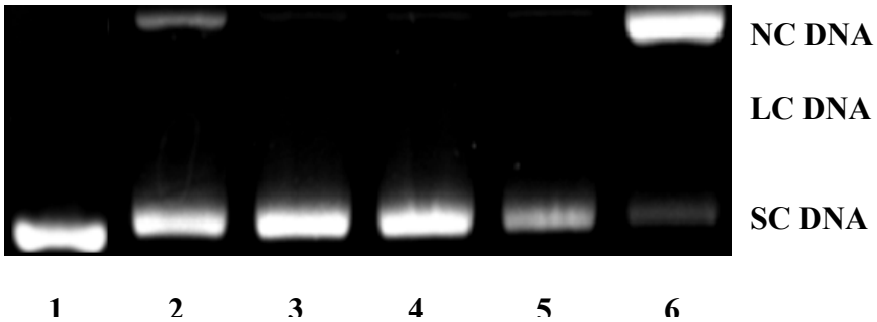

Figure S14 Gel electrophoresis diagram of cleavage of supercoiled pUC19 DNA (40 μM) by the complex **1 - 5** (30 μM) in the presence of ascorbic acid in 5 mM Tris-HCl/50 mM NaCl at pH = 7.1 and in the presence of DMSO (6 μL) at 37 ^oC. Lane 1, DNA; Lane 2, DNA + **1** + DMSO; Lane 3, DNA + **2** + DMSO; Lane 4, DNA + **3** + DMSO; Lane 5, DNA + **4** + DMSO; Lane 6, DNA + **5** + DMSO. Forms SC, NC and LC are Supercoiled, Nicked Circular and Linear Circular DNA respectively